TELKOMNIKA Indonesian Journal of Electrical Engineering
Vol. 13, No. 1, January 2015, pp. 85 ~ 90
DOI: 10.11591/telkomnika.v13i1.6760

A Novel Compact Microstrip Lowpass Filter with Sharp Transition and Improved Stopband

Pingjuan Zhang*[1], Minquan Li[2]
[1]Mathmatics and Information Engineering Institute of Anhui Science and Technology University, Fengyang 233100, Anhui, China
[2]School of Electronics and Information Engineering, Anhui University, Hefei 230039, Anhui, China
*Corresponding author, e-mail: limq@ahu.edu.cn

Abstract

A novel compact microstrip lowpass filter (LPF) is proposed in this paper, which consists of the complementary rectangle split ring defected microstrip structure (CRSR-DMS), open stubs, spurline and the dumbbell-shaped defected ground structure (DGS). Due to the unique response of the presented CRSR-DMS, a low passband insertion loss and a sharp transition of the proposed LPF was achieved. Meanwhile, an improved stopband was obtained by properly adjusting the working frequencies of open stubs, a third-order LPF using spurline and dumbbell-shaped DGS. The measured result of the designed LPF shows that attenuation rate reaches 159 dB/GHz and a wide stopband is obtained from 4.07 GHz to more than 15 GHz.

Keywords*: lowpass filter, defected microstrip structure, defected ground structure*

1. Introduction

Microstrip lowpass filter (LPF) with a small circuit size, sharp transition and wide stopband has been highly required in many microwave communication systems to block harmonic and spurious response caused by the front-end circuits [1]. Conventional microstrip line based LPFs can only provide a gradual transition and narrow upper stopband bandwidth. To sharpen attenuation rate and widen upper stopband bandwidth, many planar resonators, such as circular hairpin resonator [2] and compound resonator [3], have been developed. Another method to design compact and high-performance LPF is to employ defected ground structure (DGS) [4-12] due to its prominent stopband and obvious slow-wave effect.

Since each DGS unit can generate an attenuation pole, a wide stopband of LPF is obtained by utilizing cascaded DGS units with different lengths [4-5]. Through use of additional open stubs, stopband bandwidth may be further improved [6-7]. However, the implemented LPF often has a large physical size. Using novel shaped DGS with more attenuation poles [8-9] may effectively solve the problem. The compact LPF may also be designed based on the equivalent series inductance produced by the DGS resonator and the conventional design theory of prototype filter [10-13]. The design process of a five-pole LPF using dumbbell-shaped DGS is presented in [11] and the systematic design method for the complex DGS slot based LPF is validated in [12]. For the design of compact and high-performance LPF, multilayer technique will be a good candidate. For instance, in order to achieve a wide rejection in the stopband, two cascaded λ/2 defected microstrip structure (DMS) resonators together with two vertically located DGS resonators are employed in [13]. However, sharpness of the transition region and suppression of harmonics in the stopband need further improvement for the presented filters in [10-13].

In this paper, we propose a new compact LPF with sharp transition and improved stopband. Sharp transition and good passband performance of the LPF is obtained by using the presented complementary rectangle split ring DMS (CRSR-DMS). The improved stopband may be achieved as follows. First, two open stubs are placed in the microstrip line to generate two transmission zeros in transmission response. A third-order LPF using the spurline is then inserted in the proposed filter for wide attenuation bandwidth. Finally, two dumbbell-shaped DGSs with different lengths are employed to further widen the stopband bandwidth. The proposed filter features compactness because of its unique configuration and slow-wave effects

Received September 29, 2014; Revised November 19, 2014; Accepted December 5, 2014

of the employed resonators. Based on aforementioned design principles, the proposed LPF is implemented and its simulation and measurement results are presented.

2. Design and Implementation of the Novel Lowpass Filter

2.1. Configuration and Design of the Proposed LPF

The configuration of the proposed LPF is shown in Figure 1, where multilayer technique is used. In the top microstrip plane, two CRSR-DMSs are etched near input/output ports to produce initial two transmission zeros. Since the presented CRSR-DMS exhibits high attenuation rate and low insertion loss in the passband, which will be seen in the following section, sharp transition and good passband performance of the proposed LPF can be achieved. Two open stubs are placed near the CRSR-DMSs, resulting in another two transmission zeros. A third-order LPF using spurline is located in the middle of the microstrip line and its stopband is adopted to widen rejection bandwidth of the proposed filter. In the bottom ground plane, two dumbbell-shaped DGSs with different lengths are put below the open stubs for better harmonics suppression. By adjusting above operated frequencies properly, the extended stopband may be easily obtained without affecting the original sharp transition and good passband performance for the proposed filter.

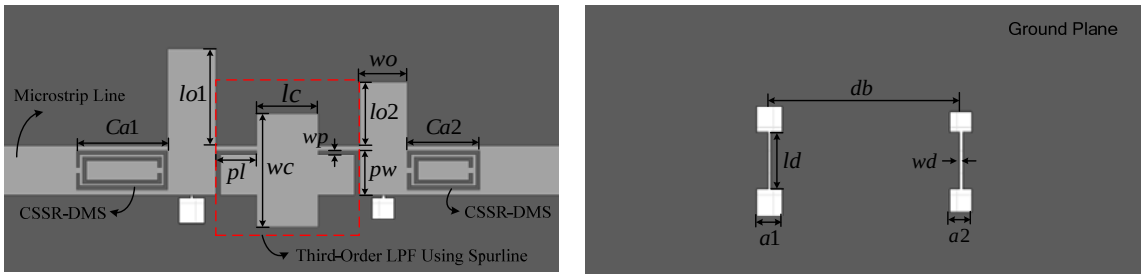

(a) Top View (b) Bottom View

Figure 1. Configuration of the proposed LPF

2.2. Characteristic of the CRSR-DMS Unit

The layout of the presented CRSR-DMS unit is depicted in Figure 2, where two concentric split ring slots with splits on opposite sides are etched in the microstrip line. Considering the limited microstrip width in practical applications, the rectangle split ring is adopted instead of the conventional square split ring. The width of the slot Cw and the distance between inner and outer rectangle split ring Cd are chosen as the same value 0.3 mm for design simplicity. The substrate used in the simulations and fabrication is Arlon Cuclad 250(tm) with a relative dielectric constant of 2.55 and a thickness of 1.5 mm. The width of the microstrip line W is chosen to be 4.5 mm corresponding to a characteristic impedance of 50 Ω. The length of the splits Cg is set as 0.6 mm.

Figure 3 shows simulated transmission responses of the CSSR-DMS unit with different lengths Ca and widths Cb. It can be clearly seen that the CSSR-DMS unit has sharp attenuation rate and little insertion loss in the passband. Moreover, it can provide two obvious attenuation poles. The superior characteristic of the presented CSSR-DMS is very helpful for the implementation of high-performance LPF. We could also find that for a fixed Ca or Cb, both resonant frequencies at the attenuation poles decrease when Cb or Ca increases. Furthermore, the insertion loss of the passband between the two attenuation poles slightly increases when Cb increases, which is good for harmonics suppression of LPF.

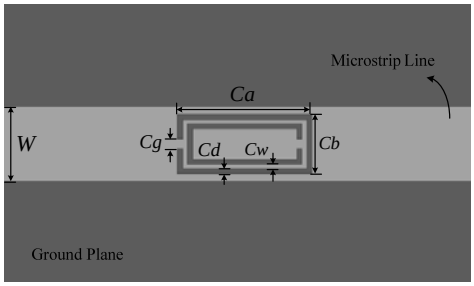

Figure 2. Layout of the CRSR-DMS unit

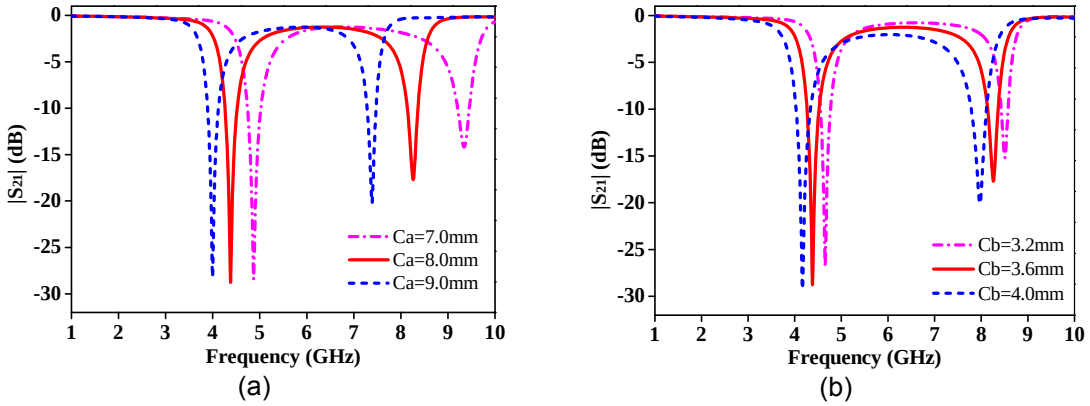

Figure 2. Effects of the length Ca (Cb=3.6 mm) (a) and the width Cb (Ca=8.0 mm) (b) on the transmission response of the CRSR-DMS

2.3. Third-Order LPF Using Spurline

The spurline with its inherently compact layout is realized by etching a folded slot in the microstrip line. Similar with the defected structures, the spurline can also provide excellent stopband [14-15]. It is noticed that the frequency response of the spurline may be represented by a parallel LC circuit with the circuit parameters computed from following expressions:

$$C = \frac{f_c}{2\pi Z_0 \left(f_0^2 - f_c^2 \right)}, \qquad L = \frac{1}{4\pi^2 f_0^2 C} \tag{1}$$

Where f_c is the 3-dB cut-off frequency, f_0 is the frequency of the attenuation pole and Z_0 is the characteristic impedance of the microstrip line.

The equivalent inductance L and capacitance C of the spurline depends on the dimensions of the defected slot. As shown in Figure 4(a), when the width pw and slot width wp are fixed to be 3.8 mm and 0.4 mm respectively, the equivalent L is proportional to the length pl while the equivalent C keeps nearly unchanged. In Figure 4(b), when the length pl and the width pw is set to be 5.0 mm and 3.0 mm correspondingly, the equivalent L slightly increases while the equivalent C decreases rapidly as the slot width wp increases. Therefore, the required circuit parameters may be easily obtained by tuning the dimensions of the spurline. Based on the filter design theory [1], a third-order LPF is designed and its configuration can be found in Figure 1(a). Two spurlines with the same size are used to construct the lumped inductance elements and the cross-junction opened stub is adopted to realize the shunt capacitance.

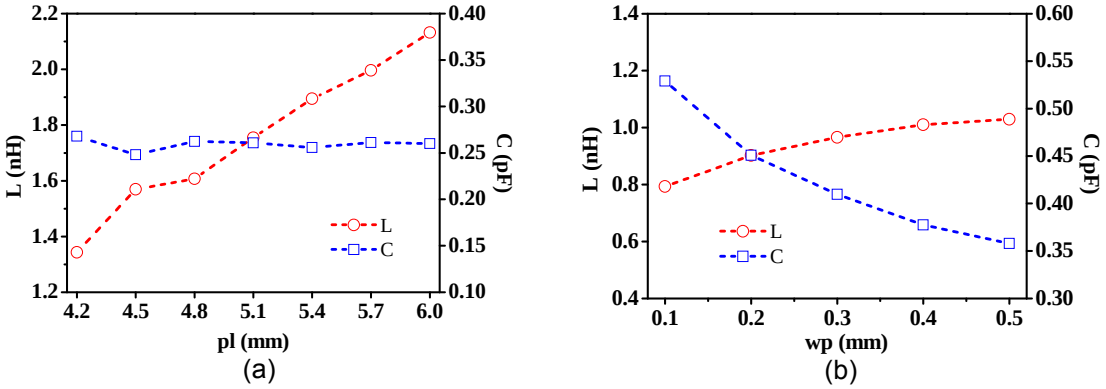

Figure 4. Equivalent L-C value versus the length pl (a) and the width wp of the spurline

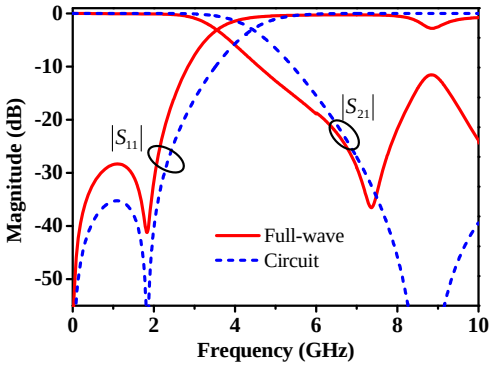

Figure 5. Full-wave and circuit simulated S-parameters of the third-order LPF using spurline

The dimensions of this third-order LPF are: pl=3.6 mm, pw=4.1 mm, wp=0.4 mm, wc=10.2 mm, lc=5.35 mm. Figure. 5 plots the circuit and full-wave simulated results and a good agreement between the two can be seen. The discrepancy at the stopband is resulted from the distributed effects and the radiation loss which are not considered in ideal circuit simulation. As shown in Figure. 5, the 20-dB rejection band is from 6.2 GHz to 8.1 GHz with an attenuation pole at 7.36 GHz. A local peak occurs around 9.0 GHz in the full-wave simulation but it has no effective bandwidth and may be suppressed by a dumbbell-shaped DGS. Due to the compact layout and good rejection characteristic of the third-order LPF, it is embedded in our proposed filter for improved stopband.

3. Experimental Validation

The proposed LPF shown in Figure 1 is designed based on previous investigations. The final optimized physical dimensions of the filter are: Ca1=8.0 mm, Ca2=6.3 mm, Cg=0.6 mm, Cw=Cd=0.3 mm, Cb=3.6 mm, wo=4.2 mm, lo1=8.8 mm, lo2=5.8 mm, wd=0.3 mm, ld=5.0 mm, a1=2.3 mm, a2=1.9 mm, db=14.65 mm, while the spurlines and the open stubs have the same specification as in Figure 5.

To better illustrate the working principle of the proposed filter, the comparison of the simulated transmission response results of CRSR-open stub, CRSR-open stub-spurline and the proposed LPF are conducted and shown in Figure 6. It is found that when there is only two CRSR-DMSs and two open stubs, six transmission zeros (4.32/5.33/5.47/7.35/8.32/10.19 GHz) are produced and a sharp transition is achieved. As the third-order LPF using spurline is embedded, the 20-dB rejection band reaches up to 10.39 GHz except a small peak around 9.0 GHz. By inserting additional two dumbbell-shaped DGSs, a deeper and wider stopband is obtained and the simulated 20-dB stopband is from 4.25 GHz to more than 15.0 GHz. It is also

found from Figure 6 that the improved stopband is realized without affecting the sharp transition and low insertion loss of the passband.

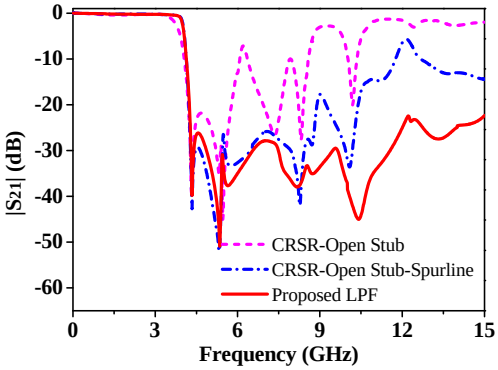

Figure 6. Simulated transmission response results of CRSR-open stub, CRSR-open stub-spurline and the proposed filter

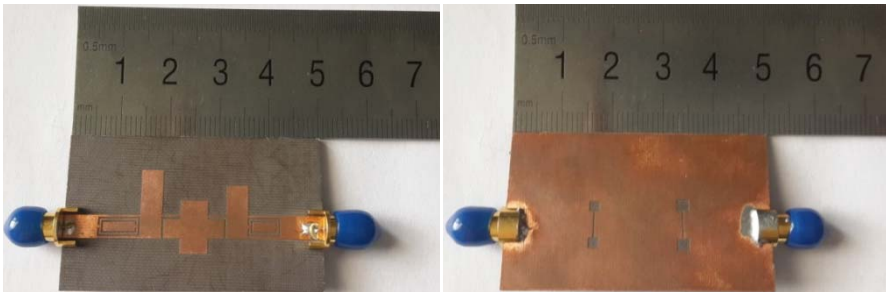

Figure 7. Photograph of the fabricated LPF

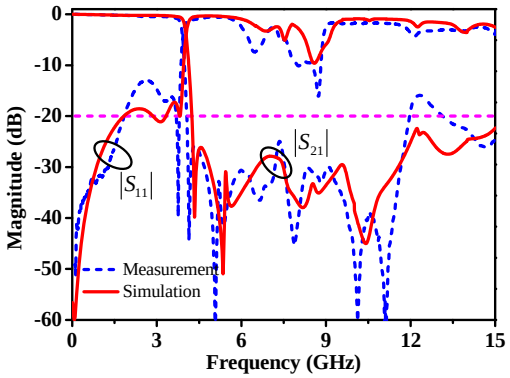

Figure 8. Simulated and measured S-parameters of the fabricated LPF

The photograph of the fabricated LPF is shown in Figure 7. The simulated frequency response result agrees well with the measured result as depicted in Figure 8 and a slight difference between the simulation and measurement is due to the fabrication tolerance. As expected, the measured result shows that the proposed LPF provides a sharp transition band from 3.88 GHz to 4.14 GHz with 3 dB and 44.35 dB rejection respectively, resulting in an attenuation rate of 159 dB/GHz. The suppression level above 20 dB is from 4.07 GHz to more than 15 GHz in spite of a small peak at 12.3 GHz. In the passband from dc to 2.06 GHz, the

insertion loss is less than 0.3 dB. The return loss is below -12.5 dB in the whole passband. In addition, the actual occupied physical area of the proposed filter is only 35.25* 16.15 mm^2.

4. Conclusion

A novel microstrip LPF with sharp transition and improved stopband is proposed and its design procedure is described. By using the presented CRSR-DMS resonator, the proposed LPF enables sharp attenuation rate and low insertion loss of the passband. Meanwhile, harmonic response of the proposed filter is effectively suppressed by open stubs, a third-order LPF using spurline and the dumbbell-shaped DGS. The measured result of the fabricated LPF shows that attenuation rate reaches 159 dB/GHz and a wide stopband is achieved. With good passband and stopband performance, simple design procedure and a compact size, the proposed LPF makes itself useful for applications in modern communication systems.

References

[1] Hong J, Lancaster M. *Microstrip Filters for RF/Microwave Applications*. New York: Wiley, 2001: 30-121.
[2] Yang M, Xu J, Zhao Q, Peng L, Li G. Compact Broad-Stopband Lowpass Filters Using Sirs-loaded Circular Hairpin Resonators. *Progress In Electromagnetics Research*. 2010; 102: 95-106.
[3] Karimi G, Lalbakhsh A, Siahkamari H. Design of Sharp Roll-Off Lowpass Ffilter with Ultra wide Stopband. *IEEE Microw. Wireless Compon. Lett.* 2013; 23(6): 303–305.
[4] Liu H, Li Z, Sun X, Mao J. An Improved 1D Periodic Defected Ground Structure for Microstrip Line. *IEEE Microw. Wireless Compon. Lett.* 2014; 14(4): 180–182.
[5] Ruiz J, L.Martinez F, Hinojosa J. Novel Compact Wide-Band EBG Structure Based on Tapered 1-D Koch Fractal Patterns. *IEEE Antennas Wireless Propag. Lett.* 2011; 10: 1104–1107.
[6] Zeng H, Wang G, Zhang C, Zhu L. Compact Microstrip Low-pass Filter Using Complementary Split Ring Resonators with Ultra-wide Stopband and High Selectivity. *Microw. Opt. Technol. Lett.* 2010; 52(2): 430–433.
[7] Tamasi M, Santanu D, Susanta P. Design and Validation of Low-pass Filter Using Microstrip Stub and Defected Ground Structure. *Microw. Opt. Technol. Lett.* 2013; 55(3): 571–573.
[8] Wang C, Lin T. A Multi-Band Meandered Slotted-Ground Plane Resonator and Its Application of Low-pass Filter. *Progress In Electromagnetics Research*. 2011; 120: 249-262.
[9] Taher H. Ultrawide Stopband Low-pass Filter Using Triangular Resonators Defected Ground. *Journal of Electromagnetic Waves and Applications*. 2014; 28(5): 542-550.
[10] Ahn D, Park J, Kim C, Kim J, Qian Y, Itoh T. A Design of theLow-pass Filter Using the Novel Microstrip Defected Ground Structure. *IEEE Trans. Microw. Theory Tech.* 2001; 49(1): 86–93.
[11] Lim J, Kim C, Ahn D, Jeong Y, Nam S. Design of Low-pass Filters Using Defected Ground Structure. *IEEE Trans. Microw. Theory Tech.* 2005; 53(8): 2539-2545.
[12] Verma A, Kumar A. Design of Low-pass Filters Using Some Defected Ground Structures. *AEU - International Journal of Electronics and Communications*. 2011; 65(10): 864-872.
[13] Boutejdar A, Omar A, Burte E. High-performance Wide Stop Band Low-pass Filter Using a Vertically Coupled DGS-DMS-Resonators and Interdigital Capacitor. *Microw. Opt. Technol. Lett.* 2014; 56(1): 87–91.
[14] Nguyen F, Chang K. On the Analysis and Design of Spurline Bandstop Filters. *IEEE Trans. Microw. Theory Tech.* 1985; 33(12):1416-1421.
[15] Tu W, Chang K. Compact Microstrip Bandstop Filter Using Open Stub and Spurline. *IEEE Microw. Wireless Compon. Lett.* 2005; 15(4): 268-270.